

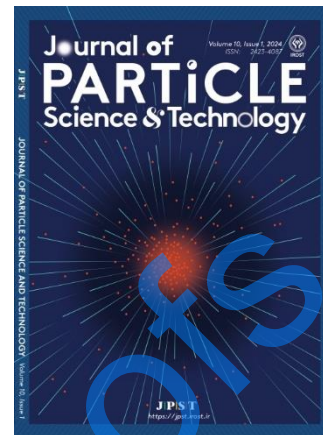
## Journal Pre-proofs

Effect of the smallest microwave-synthesized Cu<sub>2</sub>S nanoparticles with surfactant templates on improving the properties of engine oil

Azar Bagheri Gh., Forogh Nejadi, Melika Pejman

DOI: <https://doi.org/10.22104/jpst.2026.7962.1286>

Manuscript number: JPST-2510-1286



To appear in: *Journal of Particle Science and Technology (JPST)*

Received Date: 26 October 2025

Received Date in revised form: 8 January 2026

Accepted Date: 25 February 2026

**Please cite this article as:** Bagheri Gh., A., Nejadi, F., Pejman, M., Effect of the smallest microwave-synthesized Cu<sub>2</sub>S nanoparticles with surfactant templates on improving the properties of engine oil, *Journal of Particle Science and Technology* (2025), doi: <https://doi.org/10.22104/jpst.2026.7962.1286>

File of an article that has undergone enhancements after acceptance, such as the addition of a cover page and metadata, and formatting for readability, but it is not yet the definitive version of record. This version will undergo additional copyediting, typesetting and review before it is published in its final form, but we are providing this version to give early visibility of the article. Please note that, during the production process, errors may be discovered which could affect the content, and all legal disclaimers that apply to the journal pertain.

© 2025 The Author(s). Published by [IROST](#).

## Effect of the smallest microwave-synthesized Cu<sub>2</sub>S nanoparticles with surfactant templates on improving the properties of engine oil

Azar Bagheri Gh.<sup>1</sup>, Forogh Nejadi<sup>1</sup>, Melika Pejman<sup>2</sup>

<sup>1</sup> Department of Chemistry, Central Tehran Branch, Islamic Azad University, Tehran, Iran

<sup>2</sup> Faculty of Medicine, Iran University of Medical Sciences, Tehran, Iran

### Abstract

In this study, the preparation and identification of Cu<sub>2</sub>S nanoparticle was carried out using the microwave method, and the effect of irradiation time, power, and surfactant on particle size was investigated. The sample was characterized by XRD measurements, field emission scanning electron microscopy (FE-SEM), Fourier transform infrared (FT-IR), and ultraviolet-visible (UV-vis). Also, the results of FE-SEM on nanoparticles prepared with four surfactants, EDTA, sorbitol, citric acid and PEG400 showed that nanoparticles synthesized with PEG400 surfactant have the smallest size. Then, the effect of microwave power on the size of Cu<sub>2</sub>S nanoparticles was investigated at three powers of 700, 500 and 900 W. And the FE-SEM results showed that Cu<sub>2</sub>S nanoparticles have the smallest size at 500 W. To investigate the effect of time on the size of Cu<sub>2</sub>S nanoparticles, the experiments were repeated at times of 3, 5 and 10 minutes, and the FE-SEM results obtained from this stage showed that after 10 minutes, Cu<sub>2</sub>S nanoparticles have the smallest size. Also, the effects of the prepared Cu<sub>2</sub>S nanoparticles on the thermal conductivity (*K*), density and viscosity of engine oil were investigated. The results obtained from this research show that the increase in thermal conductivity compared to the base oil indicates that these nanoparticles improve the heat transfer ability and operation of engine oil in harsher temperature conditions.

**Keywords:** Cu<sub>2</sub>S Nanoparticle; Engine oil; Surfactant; Microwave method

## 1. Introduction

Engine oil has reciprocal effects such as reducing the amount of friction between parts and engine coolant. One of the methods of further reducing friction inside the engine can be done by distributing nanoparticles in the engine oil. Considering the role of nanoparticles as fillers, their addition to engine oil causes filling of the impure surfaces of engine components and reducing the effect of friction and wear, and consequently lowering the engine temperature. This effect of nanoparticles, together with the lubricating role of engine oil, reduces fuel consumption and exhaust pollutants in vehicles.

By moving from microparticles to nanoparticles, we encounter changes in some physical properties, two of which are the increase in the surface area to volume ratio and the entry of particle size into the realm of quantum effects. The increase in the surface area to volume ratio that occurs gradually with the decrease in particle size causes the behavior of atoms located on the particle surface to prevail over the behavior of internal atoms. This phenomenon affects the properties of the particle in isolation and its interactions with other materials. Increasing the surface area greatly increases the reactivity of nanoparticles because the number of molecules or atoms present on the surface is very large compared to the number of atoms or molecules present in the bulk of the sample, such that these particles have a strong tendency to agglomerate [1]. Researchers conducted numerical and experimental investigations on the fluid flow and heat transfer properties of several nanofluids comprising SiO<sub>2</sub> [2], ZnO [3], CuO [4], Al<sub>2</sub>O<sub>3</sub> [5,6], and silver [7] nanoparticles. They evaluated characteristics such as viscosity, thermal conductivity, and the impacts of viscous dissipation.

The nanoparticles examined in this study are copper sulfide [8-11], which is due to its excellent properties, including strong thermal conductivity Cu<sub>2</sub>S (chalcocite) is a p-type semiconductor which lies in an optimum range for solar energy conversion [12], solar cells [13], catalysis [14], efficient photo catalyst [15], biosensors [16] and potential applications in optoelectronics devices [17]. Hence, efforts

were made to find out new methods for the synthesis of  $\text{Cu}_2\text{S}$  nanostructures with different morphologies such as nanoparticles [18], nanowires [19], nano plates [13] and can be synthesized by different methods such as sonochemical [20], microwave [21], hydrothermal, and sol-gel [22]. Nowadays, template-assisted methods for nano materials (NMs) synthesis are an emerging field for researchers. These methods enable precise control over the morphology, dimensions, composition, and enhanced properties of NMs [23-26]. The physical and chemical properties of NMs can vary significantly depending on the type of surfactants [27]. Many efforts have been devoted to designing of novel synthetic route to fabricate  $\text{Cu}_2\text{S}$  nanostructures with controlled shape and size. In 2003, Liao and his colleagues successfully prepared copper sulfide nanorods using a microwave method in 20 minutes at a power of 650 W [9]. These nanorods had a diameter of 5-10 nm. The group used sodium nitrate trihydrate and thioacetamide as starting materials and sodium dodecyl sulfate (SDS) as surfactant. In 2007, Tangtom and his colleagues were able to prepare spherical copper sulfide nanostructures using a microwave method under controlled conditions [10]. In 2010, Li and his colleagues successfully prepared clustered copper sulfide nanostructures using a solvothermal method. In this method, copper nitrate trihydrate and thiourea were used as starting materials and ethylene glycol as a solvent [11]. Double-fold snowflake copper sulfide ( $\text{Cu}_2\text{S}$ ) was prepared via a template and surfactant-free method using dimethyl sulfoxide (DMSO) as a solvent [21].

The methods of fabrication NMs have a significant impact on the properties of these materials. [28]. Conventional methods for synthesizing nanomaterials are not fast enough and environmentally friendly enough to meet the growing demand for semiconductor nanomaterials [29]. Therefore, new methods for preparing and controlling the size and shape of copper sulfide nanostructures that are rapid and environmentally safe need to be developed [30,31]. Synthesis using microwave (MW) irradiation has shown significant improvements in purity, size, and other product properties compared to traditional

heating. Microwave irradiation directly affects the composition of the mixture and converts electromagnetic energy into heat through molecular interactions, thereby providing uniform heating throughout the synthesis process [32-34]. A large number of reactions in organic and inorganic synthesis have been studied using this method. These include radioisotope synthesis [35], fullerene chemistry [36], homogeneous [37]/heterogeneous catalysis [37,38]. Many review articles have covered almost all aspects from accelerated synthesis rates, microwave effects, to microwave equipment [39–42].

Based on a literature review, there is little information examining the effect of adding nanoparticles to base fuel. In this study, the preparation and identification of  $\text{Cu}_2\text{S}$  nanostructures, were carried out by microwave method, and the effect of changing various reaction conditions, including surfactant, power and time, was investigated to achieve optimal conditions (specific size and morphology) in the preparation of nanoparticles. Then, the effect of the smallest synthesized  $\text{Cu}_2\text{S}$  nanoparticles on the thermal coefficient of engine oil and its performance was investigated.

## 2. Experimental

### 2.1. Materials

Ethanol (99.9 % Sigma Co.) were used as received, without further purification. Other compounds used were prepared from MERCK company. In this research, Behran Tarash engine oil was used.

### 2.2. Apparatus

Phase identification of the fabricated sample was carried out by a Holland Philips X-ray diffraction  $\text{CuK}\alpha$  ( $\lambda=1.5417 \text{ \AA}$ ) in the radiation range of  $20^\circ\text{--}80^\circ$ . Scanning electron microscope images were recorded by TESCAN Company model MIRA III made in the Czech Republic. The presence of surface functional groups in the prepared samples was analyzed by Fourier transform infrared spectrometer (FT-

IR) THERMO Company model AVATAR made in the United States. Spectrophotometric measurements were conducted using an UV-VIS Shimadzu 2101 spectrophotometer equipped with a Acermate 486 SX/25D computer and thermostically matched 10-mm quartz cells. A vacuum Dry Oven model made by Yamato Company is also used. Density and viscosity measurements were performed with the device - SVM3000 model - Anton Paar, made in Germany. Thermal Analyzer KD2 Model Dragon, Ultrasonic Bath Machine Rayan Sanat Technology Co. and Ultrasonic Probe-Misonix Model.

### 2.3. Synthesis of $Cu_2S$ nanostructures

Studies show MW method can produce catalyst with large surface area, pore volume, pore width as well as enhancing the crystal growth [43]. Microwave power density is an important parameter for determination of crystal structure and surface area including reduce the particle size along with band gap while generating many site defects which contribute in hindering electron-hole from recombine and aiding charge carrier migration. Also, the size of the nanoparticles has a significant role to play in their applications. The role of the irradiation time was considered as the primary concern to regulate the size and possibly the shape of the synthesized nanoparticles. In this study, the effect of various factors on particles size are investigated.

In general, Copper sulfate solution (0.01 moles) and then one of the surfactants to the test container. We adjust the pH with 1 N NaOH solution and adjust the pH to the range of 5, which results in the formation of yellow precipitates. Then, we add 0.1 M thiourea solution to the solution in the first test container and irradiate in the microwave at different powers and with a time pattern of 30 seconds on and 70 seconds off. After the sample cools, we pass the solutions through filter paper and wash the precipitates with distilled water several times. We perform the same steps for the other four surfactants [sorbitol (A1), citric acid (A2), PEG400 (A3) and EDTA (A4)].

This experiment is performed in three stages:

Step 1. Investigating the effect of surfactants on particle size and selecting the best surfactant by producing nanoparticles with the smallest size (at 600 watt and 3 minutes).

Step 2. After selecting the best surfactant, investigating the effect of power on particle size

Step 3. After selecting the best power, investigating the effect of time on particle size.

The formation mechanism of copper sulfide nanostructures is shown in (Fig. 1).

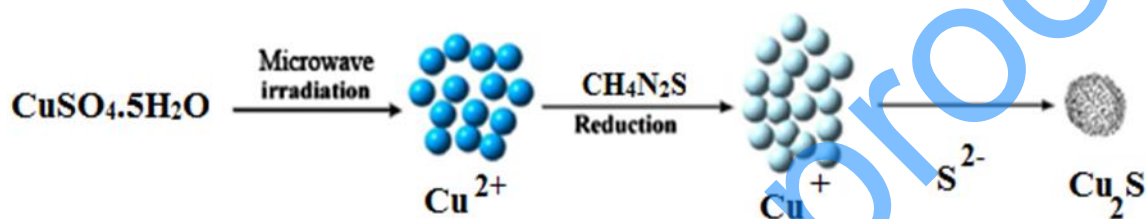


Fig. 1. Formation mechanism of copper sulfide nanostructures.

Step 2: In this step, as in the first step, we prepare solution A3 (meaning the solution before the irradiation step), then we divide the sample into three parts to conduct an experiment to investigate the effect of power on particle size with PEG400 surfactant. Then we irradiate the samples with three powers of 500 watt (B1), 700 watt (B2) and 900 watt (B3) and a time of 3 minutes. Then, as in the first step, we perform the operation of smoothing and drying the sediments and perform the FE-SEM test for the three sediments obtained.

Step 3: In this step, we prepare solution A3 (meaning the solution before the irradiation step) as in the first and second steps. Then we divide the sample into two parts to conduct an experiment to investigate the effect of time on particle size with PEG400 surfactant. Then we irradiate the samples with a power of 500 watts for two times of 5 minutes (C1) and 10 minutes (C2). Then, as in the previous steps, we perform the operation of smoothing and drying the sediments and perform the FE-SEM test for the two sediments obtained.

### 2.3. Applied experiments

#### 2.3.1. Measurement of thermal conductivity, viscosity, and density on nanofluid prepared from synthesized copper sulfide in engine oil

In this research, due to the high accuracy and high speed of the transient hot wire method, we use the KD2 Pro thermal analyzer and the KS1 sensor to determine the thermal conductivity of nanofluids.

Fig.2 KD2 shows the Pro thermal analyzer and schematic diagram of the device.

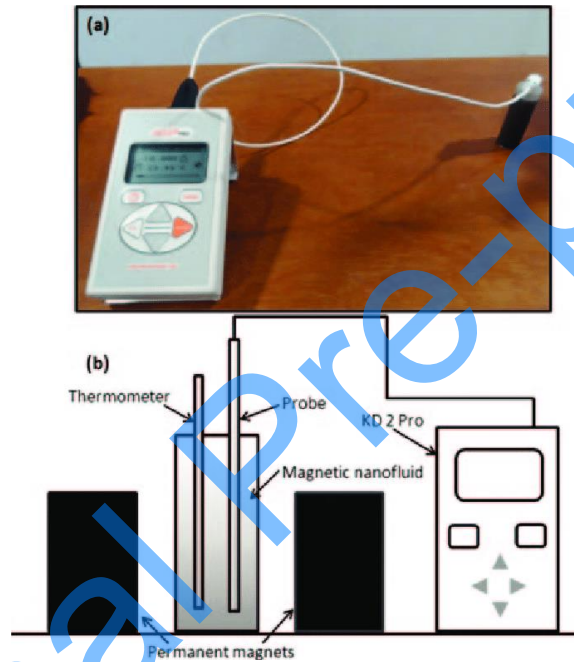


**Fig. 2.** Thermal analysis by KD2 pro.

First, we prepare 2 nanofluids with a concentration of 0.1 and 0.5 percent by weight prepared from copper sulfide nanoparticles in base oil and place each of the two nanofluid samples in a magnetic stirrer for one hour. Then, first, we disperse the copper sulfide nanoparticles in the oil in an ultrasonic bath. If the sample is not dispersed, we use ultrasonic probe for the dispersion operation to obtain a uniform nanofluid. Only the nanofluid made with a concentration of 0.5 percent by weight was dispersed with an ultrasonic probe device. At this stage, the samples are ready to perform the electrical conductivity test.

First, we measure the conductivity of the base oil as a control and then we measure the conductivity of the made nanofluids.

### 2.3.2. Viscosity and density measurement test

First, we prepare a nanofluid sample with a concentration of 0.5% by weight prepared from copper sulfide nanoparticles in engine oil and place each of the two nanofluid samples in a magnetic stirrer for one hour. Then, we first disperse the copper sulfide nanoparticles in the oil in an ultrasonic probe to obtain a uniform nanofluid. Then, the viscosity of the nanofluid was measured using an Anton Paar device, and we also measured the base oil at temperatures of 40 and 100 °C, and we also measured the density at temperatures of 15 and 40 °C.

## 3. RESULTS AND DISCUSSION

### 3.1. Structural analysis

#### 3.1.1. X-ray diffraction (XRD) results

The crystal structure and purity of the obtained product are determined by the XRD method. Figure 2 shows the X-ray diffraction pattern of the samples synthesized with different surfactants with irradiation at a power of 500 W and a temperature of 10 minutes. The peaks of this pattern are reported in the range of  $\theta$  from 10 to 80 degrees. All the peaks reported in this pattern are completely distinguishable from each other, which is in good agreement with the data reported in the articles according to Figure 3. This pattern shows broad peaks originating from the (102), (110), (103), (112) and (201) lattice plane, which are very close to those reported for hexagonal chalcocite  $\text{Cu}_2\text{S}$  (JCPDS card 26-1116) with the  $P6_3$  space group and a primitive unit cell with  $a = 3.961 \text{ \AA}$  and  $c = 6.722 \text{ \AA}$ . There is a peak at 46.74, which is a characteristic peak for  $\text{Cu}_2\text{S}$  [44]. Broadening of the peaks indicates the

nanocrystalline nature of the material. The crystallite sizes of the samples were estimated from XRD patterns and Debye–Scherrer formula:

$$D_c = K\lambda / \beta \cos\theta$$

where  $\lambda$  is X-ray wavelength ( $=1.54 \text{ \AA}$ ),  $\theta$  is the Bragg diffraction angle, and  $\beta$  is the full width in half maximum (FWHM) of the peak appearing at the diffraction angle of theta. The average crystallite diameter of the obtained products was about 9 nm.

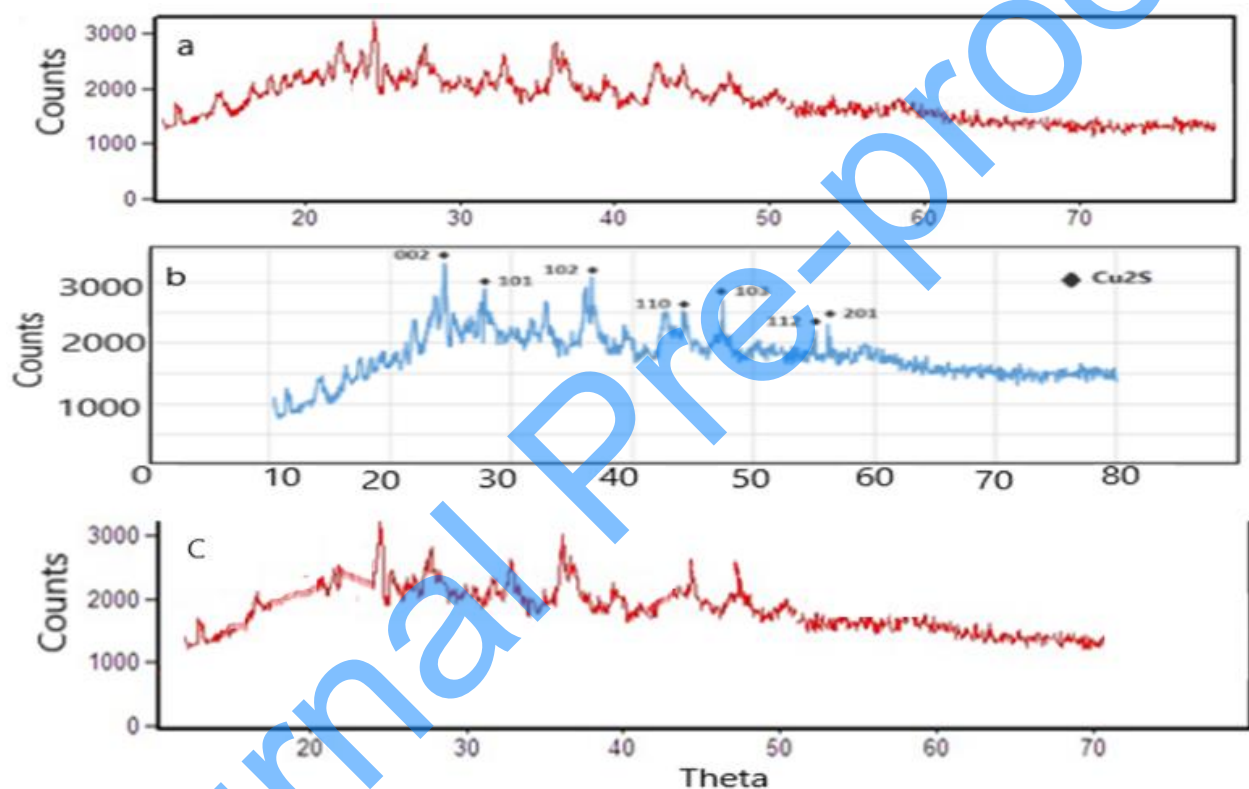


**Fig. 3.** XRD pattern of the Cu<sub>2</sub>S structure for the sample synthesized with sorbitol(a), PEG 400 (b) EDTA(c) surfactants with irradiation at 500 watts and temperature for 10 minutes.

### 3.1.2. FT-IR Spectrum

The FT-IR spectrum of nanoparticles is shown in Fig. 4. Because nanoparticles have a high surface-to-volume ratio, they absorb moisture in the laboratory and the bands related to the absorbed water are observed in their FT-IR spectrum. The band at  $3417.69 \text{ cm}^{-1}$  is related to the stretching and bending

vibrations of the (H-O) groups of water. The absorption band at  $1638.14\text{ cm}^{-1}$  and  $1103.04\text{ cm}^{-1}$  are also related to C=O and C-O bonds respectively. The band at  $1414.08\text{ cm}^{-1}$  is related to the (C-N) thiourea.

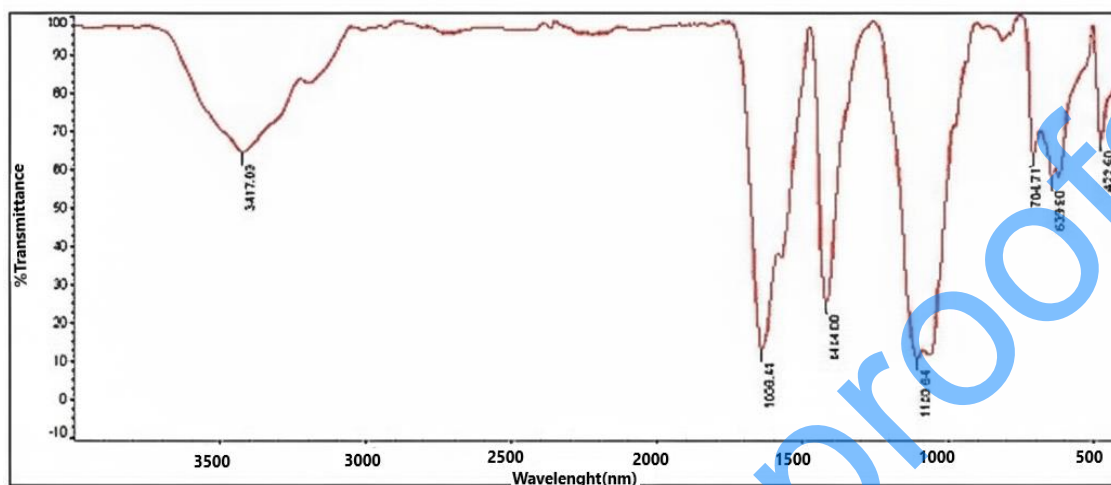


**Fig. 4.** FT-IR pattern of  $\text{Cu}_2\text{S}$  nanoparticles from the sample synthesized with PEG 400 surfactant with irradiation at 500 W and temperature for 10 minutes.

### 3.1.3. UV-Visible Spectroscopy

Fig. 5 shows the absorption spectra of  $\text{Cu}_2\text{S}$  nanostructures synthesized with different surfactants at 500 watts and 10 minutes. To obtain an absorption spectrum of copper sulfide, first weigh 0.005 grams of the sample powder and then add it to 10 cc of water as a solvent. This solution is so-called dispersed by an ultrasonic device until the distance between the nanoparticles reaches atomic size and a homogeneous and uniform solution is obtained. By doing this, the incident beams of the spectrometer will encounter a homogeneous cross-section of particles, and with this dispersion, the agglomeration of nanoparticles will be prevented to an acceptable extent, and as a result, a more desirable absorption spectrum will be obtained. In the samples in question, as shown in the figure, a sharp absorption peak is shown in the region of 190-350 nm, which, according to the existing patterns in Fig. 5 shows the formation of  $\text{Cu}_2\text{S}$  in samples  $A_1$ ,  $A_2$ , and  $A_3$ . The optical properties were measured using UV-vis spectrophotometry.

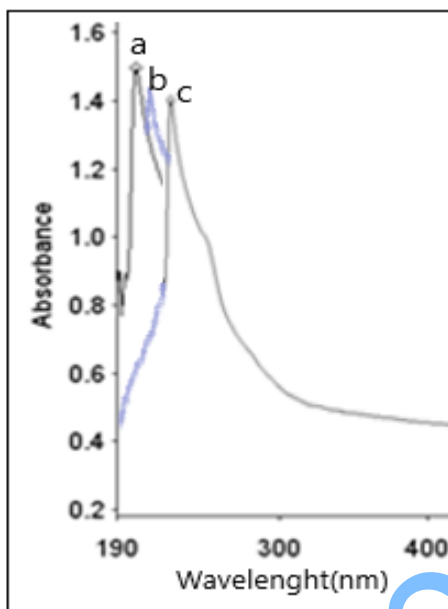


**Fig. 5.** UV-vis absorption spectrum of the Cu<sub>2</sub>S structure corresponding to sample PEG 400 (a), sorbitol (b) EDTA (c) surfactants.

Compared with bulk Cu<sub>2</sub>S, which has an absorption onset at about 1020 nm [45], the absorption edge of obtained Cu<sub>2</sub>S nanostructures exhibit a blue-shift, which is attributed to the quantum confinement of charge carriers in the nanoparticles [46].

### 3.2. Investigation of the effect of surfactant on the size of copper sulfide nanoparticles:

In this study, four surfactants were used and the results were compared under different conditions. The morphologies and microstructure of the products were further investigated by FE-SEM. The FE-SEM images show clusters comprised of nanoplates with hexagonal morphology (Figures 6-9).

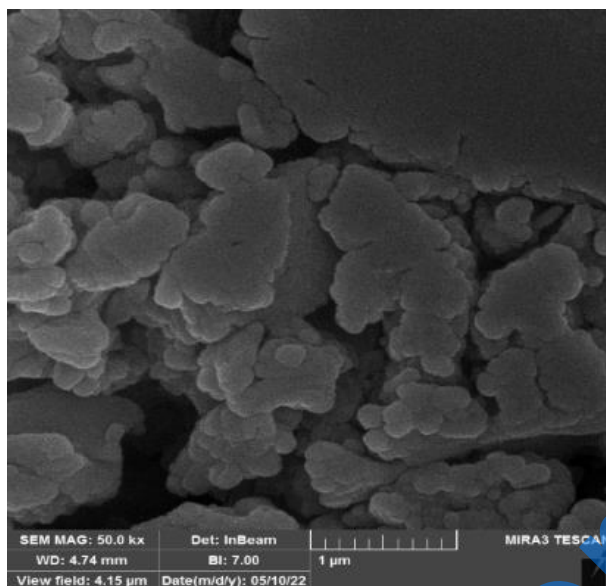


**Fig. 6.** FE-SEM images of sample A1-sorbitol surfactant - irradiated under 600 watts for 3 minutes.

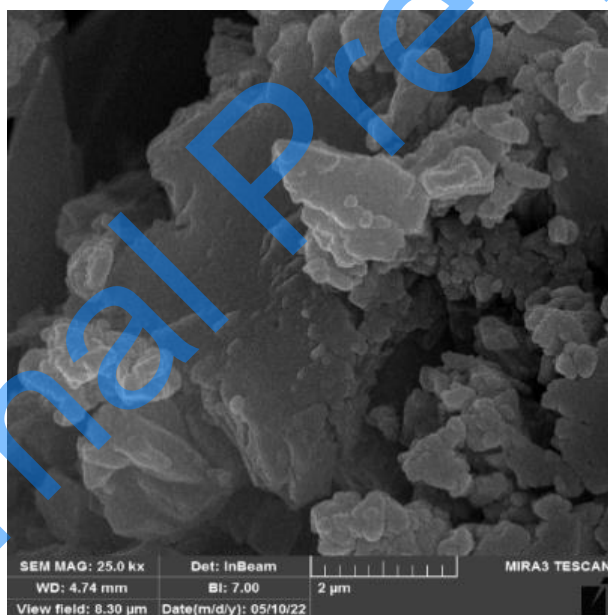


**Fig. 7.** FE-SEM images of sample A2 - citric acid surfactant - irradiated under 600 watts for 3 minutes.

### 3.3. Effect of power on the size of copper sulfide particles

To investigate the effect of power on particle size, 500, 700 and 900 W power was applied for 3 minutes. FE-SEM images obtained from the scanning electron microscope of samples B<sub>3</sub>, B<sub>2</sub>, and B<sub>1</sub>

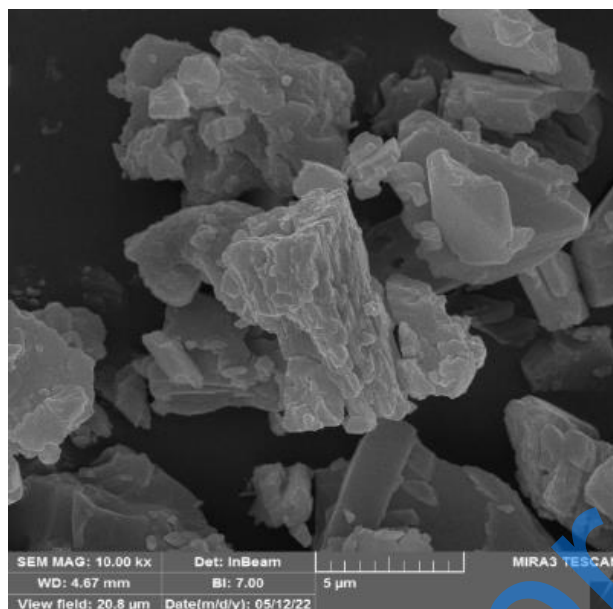


**Fig. 8.** FE-SEM images of sample A3 - PEG400 surfactant - irradiated under 600 watts for 3 minutes.

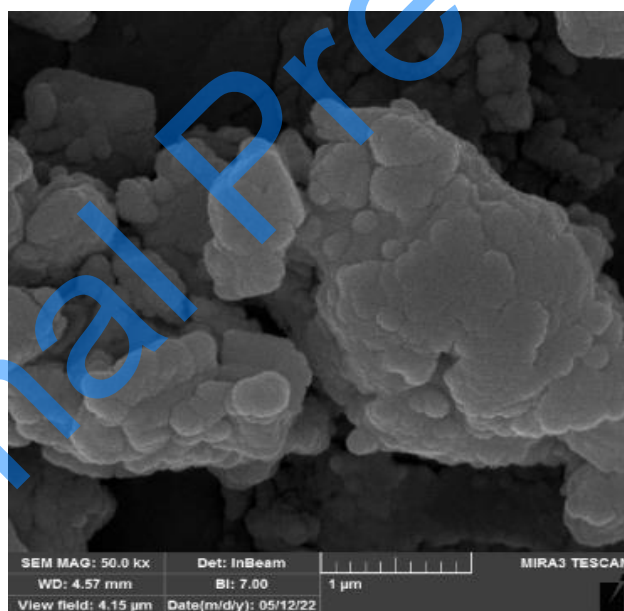


**Fig. 9.** FE-SEM images of sample A4 - EDTA surfactant - irradiated under 600 watts for 3 minutes.

(Figures 10-12) and it was concluded that the nanoparticles at the power of 500 W have a better distribution than the other two powers and the particle size is smaller than the other two powers. The

power is higher than the optimal energy for preparing copper sulfide nanoparticles, and due to the active surface of the nanoparticles, large and cohesive masses are produced from them.

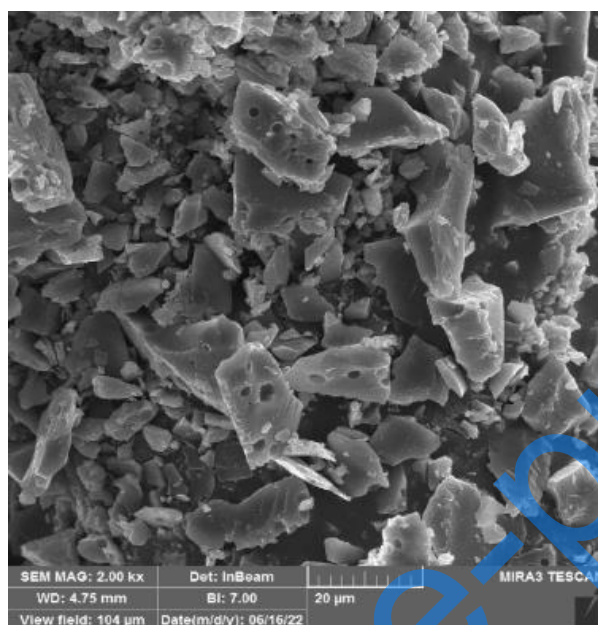


**Fig. 10.** FE-SEM images of sample B1- under 500 W power irradiated for 3 minutes.

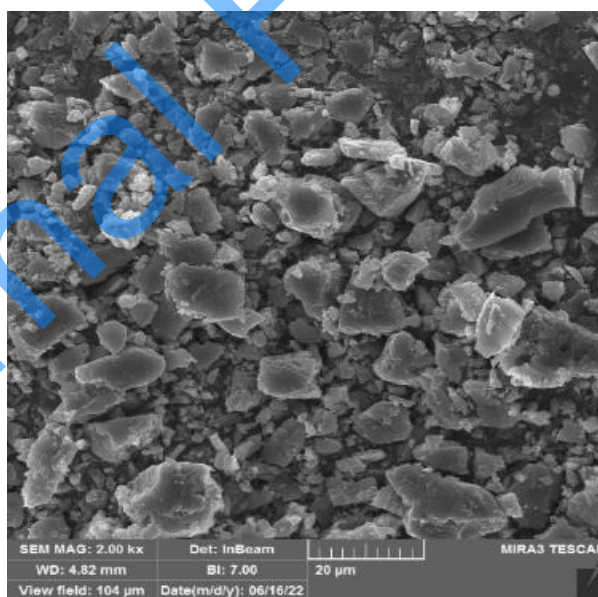


**Fig. 11.** FE-SEM images of sample B2- under 700 W power irradiated for 3 minutes.

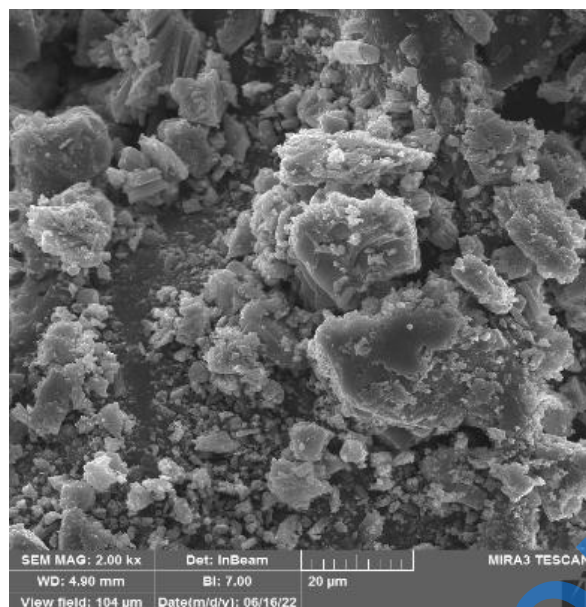


**Fig. 12.** FE-SEM images of sample B3- under 900 W power irradiated for 3 minutes.

### 3.4. Investigating the effect of time on the size of copper sulfide nanoparticles

To investigate the effect of time on particle size, studies were repeated at 3, 5, and 10 minute intervals. FES-EM images obtained from the scanning electron microscope of samples C<sub>1</sub>, C<sub>2</sub>, and B<sub>1</sub> (Figures 13 and 14).

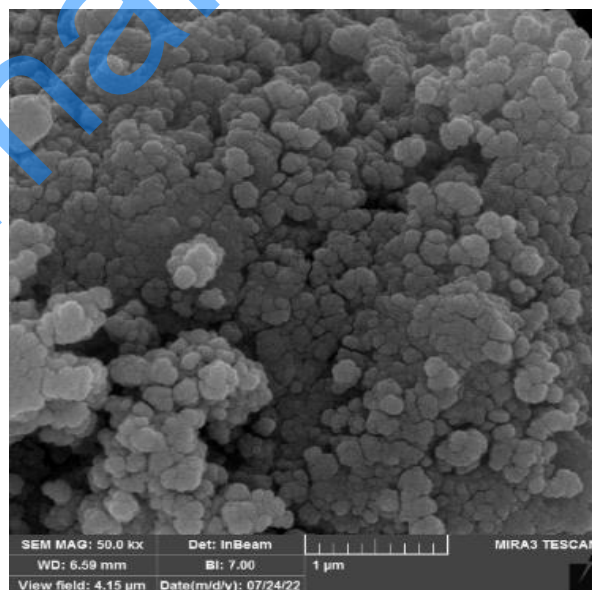


**Fig. 13.** FE-SEM images of sample C1- under 500 W power that was irradiated for 5 minutes.

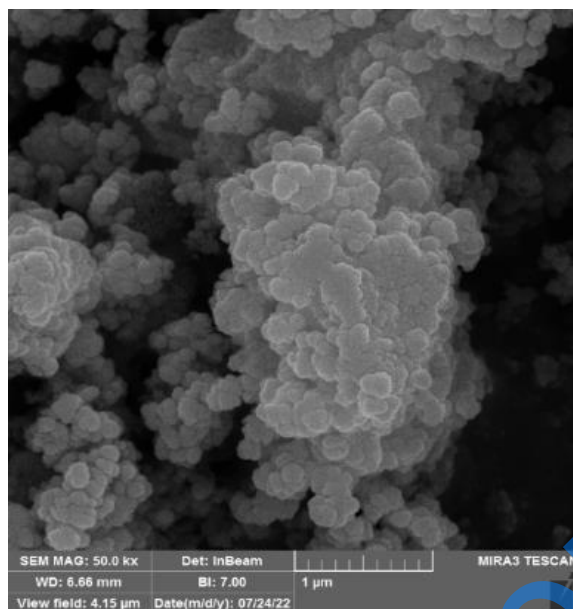


**Fig. 14.** FE-SEM images of sample C2- under 500 W power that was irradiated for 10 minutes.

### 3.5. Determining particle size using ImageJ software

Using scanning electron microscope images of the studied samples and using Image J software, the size of the nanoparticles was determined and compared (Figures 15-17).

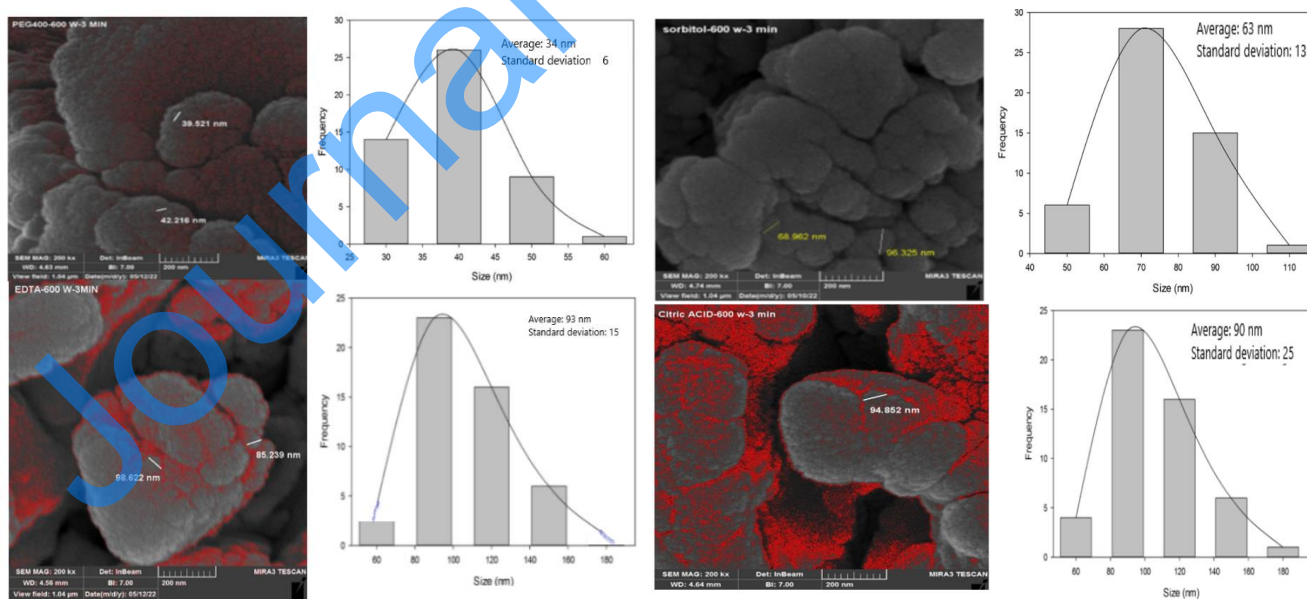


**Fig. 15.** Scanning electron microscope image of A1, A, A3 and A4 samples - Nanoparticle size analysis with ImageJ software.

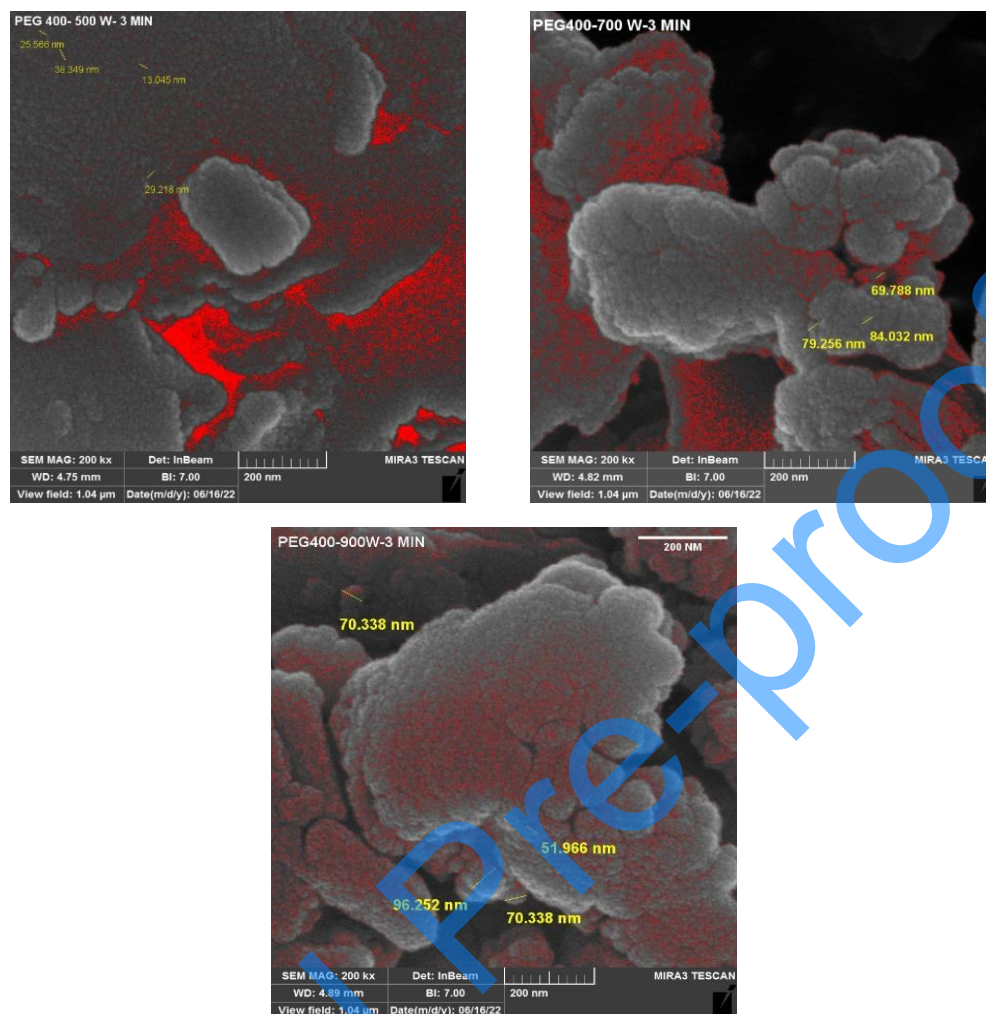


**Fig. 16.** Scanning electron microscope image of B1, B2 and B3 samples - Nanoparticle size analysis with Image J software.

According to the images obtained from the scanning electron microscope of samples A1, A2, A3, and A4, the particle size was determined and compared using ImageJ software. It was concluded that with PEG400 surfactant, better particle distribution and smaller nanoparticles were formed (Fig. 15).

According to the images obtained from the scanning electron microscope of samples B3, B2, and B1, the particles size was determined and compared using ImageJ software Fig. 16. It was concluded that the nanoparticles at the power of 500 W have a better distribution than the other two powers and the particle size is smaller than the other two powers. The power is higher than the optimal energy for

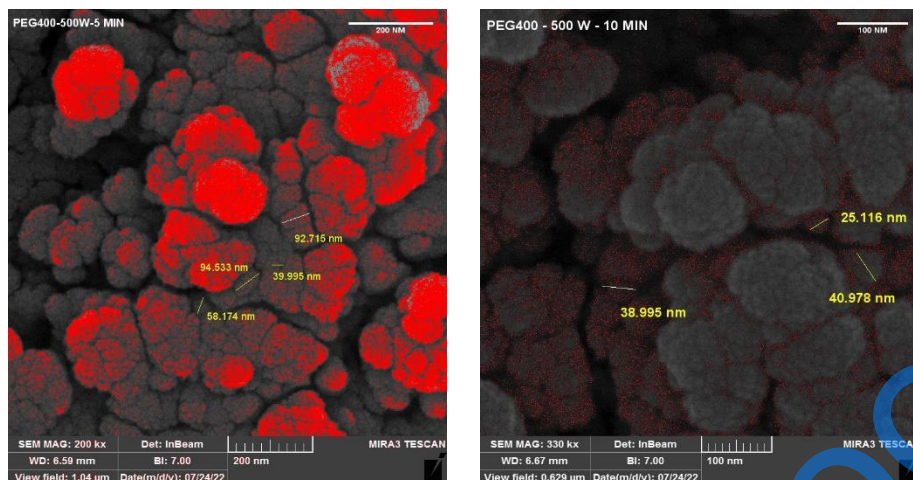


**Fig. 17.** Scanning electron microscope image of C1, C2 samples - Nanoparticle size analysis with Image J software.

copper sulfide nanoparticles, and due to the active surface of the nanoparticles, large and cohesive masses are produced from them.

According to the images obtained from the scanning electron microscope of samples C2, C1 and B1, the particle size was determined and compared using ImageJ software (Figures 16 and 17). It was concluded that at this stage, the time of 10 minutes is the best possible time due to having enough time for the formation and separation of particles.

### 3.6. Thermal conductivity measurement results

In general, nanoparticles have attracted much attention due to their significant enhancement of the thermal conductivity of fluids. Considering that metallic solids and their oxides, as well as carbon structures, have higher conductivity than fluids, the idea of dispersing solid particles in fluids to increase fluid conductivity was born by Eastman and Koblinsky. They consider the main factor effective in the abnormal increase in the conductivity of nanofluids to be effective, which can be used to explain the abnormal behavior of nanofluids. Here, we will only mention a few of these: 1-Brownian motion of

nanoparticles, 2-Nanolayers formed at the boundary between nanoparticles and the base fluid, 3-Nature of heat transfer in nanoparticles and investigation of phonon transport, and 4-Effect of nanoparticle clustering.

Thermal conductivity measurement results of base oil (Behran oil), nanofluids made of copper sulfide nanoparticles in Behran oil with a concentration of 0.1 and 0.5 weight percent. The results of measuring the thermal conductivity of the base oil and the nanofluids prepared in this study at a concentration of 0.1 % (L) and 0.5 % (H) by weight are shown in Fig. 18. As can be seen, the thermal conductivity coefficients have increased by an average of 3% compared to the base oil.

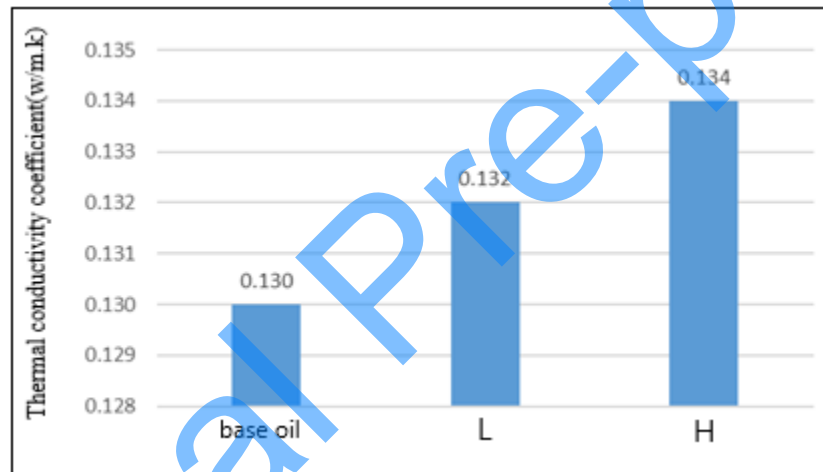


**Fig.18.** comparison of the thermal conductivity coefficients of nanofluid prepared from copper sulfide with base oil at concentrations of 0.1 and 0.5 wt%.

Results of measuring viscosity at two temperatures of 40 and 100 °C for 0.5 % by weight nanofluid made of copper sulfide in base oil and base oil (Table 1, Figure 19). Adding 0.5 % by weight of copper sulfide nanoparticles to the base oil increased the viscosity by 0.18 % at 40 °C and by 0.67 % at 100 °C. As expected, the viscosity of all samples decreased with increasing temperature. When spherical

nanoparticles are added to the oil, the nanoparticles are placed between the oil layers and slightly reduce the ease of movement of the fluid layers over each other, resulting in a slight increase in viscosity.

**Table 1.** Viscosity measurement at two temperatures of 40 and 100 °C for 0.5 % by weight copper sulfide nanofluid in Behran oil.

Sample specifications	Viscosity @ 40°C	Viscosity @ 100°C	Unit
Base oil	23.36	4.628	mm <sup>2</sup> /s
Nanofluid 5 % by weight	23.95	4.789	mm <sup>2</sup> /s

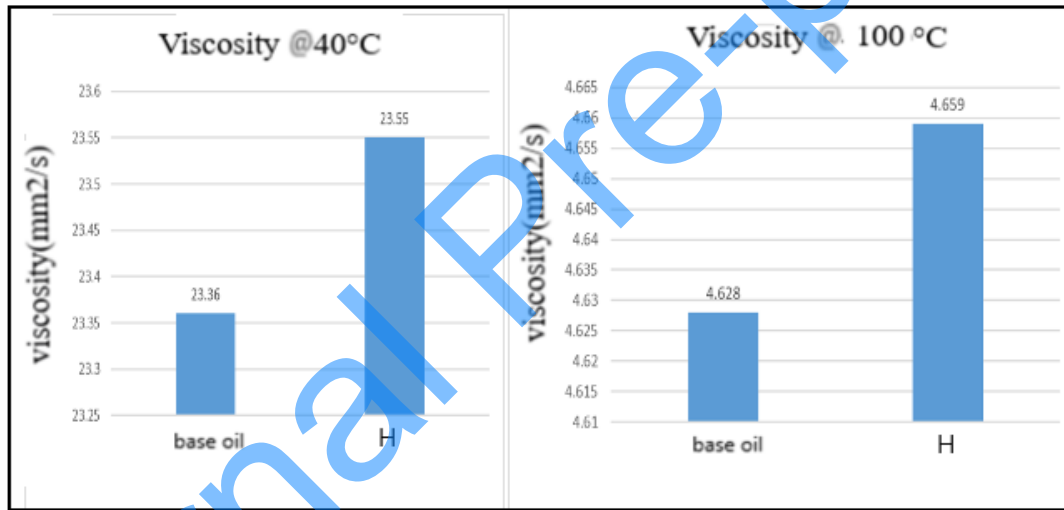


**Fig.19.** Comparison of the viscosity of base oil and nanofluids made from copper sulfide nanoparticles with a concentration of 0.5% by weight at temperatures of 100 and 40°C.

The density of base oil and nanofluids made from copper sulfide nanoparticles with a concentration of 0.5 % by weight was investigated and compared at temperatures of 15 and 40 °C. The results are shown in Table 2 and Fig. 20. According to the results, the density increased by 0.0 3% at 15 °C and by 0.02 % at 40 °C.

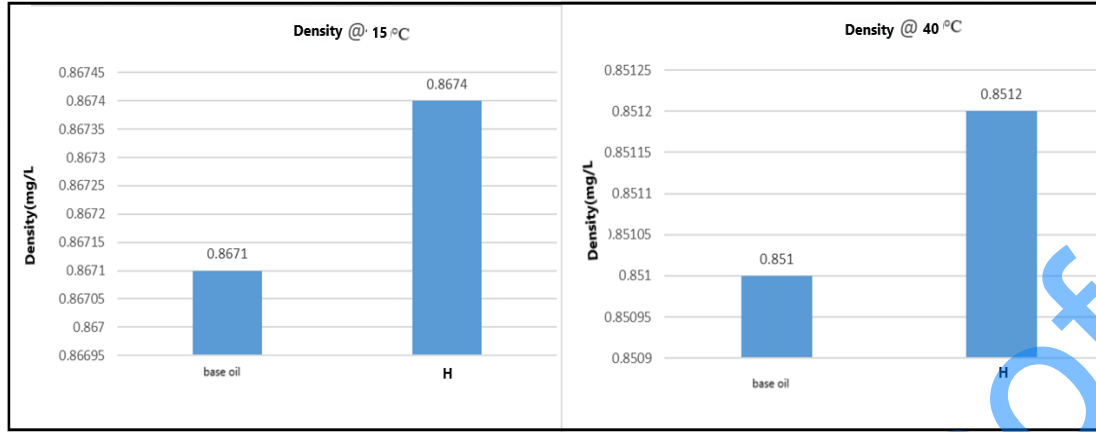


**Fig. 20.** Comparison of the density of base oil and nanofluids made from copper sulfide nanoparticles with a concentration of 0.5% by weight at temperatures of 15 and 40 °C.

**Table 2.** Density measurement at two temperatures of 15 and 40 °C for 0.5 % by weight nanofluid.

Sample specifications	Density @ 40°C	Density @ 100°C	Unit
Base oil	0.8671	0.8510	g/ml
Nanofluid 0.5 % by weight	0.8778	0.8865	g/ml

High oil temperature accelerates the oxidation rate of the base oil, so that according to the Arrhenius equations, for every 10 °C increase in the operating temperature of the oil, the oxidation rate of the oil doubles, causing its viscosity to increase. Also, the base oil contains light and volatile substances that evaporate if the temperature exceeds the allowable limit, causing the viscosity of the oil to increase. Therefore, it can be said that increasing the thermal conductivity of the in order to increase its resistance to temperature increases is an important parameter in improving its performance.

#### 4. Conclusion

Nanofluids exhibit higher stability compared to traditional fluids due to the size-dependent phenomenon and random motion of nanoparticles known as Brownian motion. The ultrafine shape of

nanoparticles enables unrestricted fluid flow in a microchannel, resulting in smoother flow. The use of nanoparticles increases engine performance for several reasons:

1. Reducing the size of the thermal transfer system, which increases with the increase in the energy density of nanoparticles, and consequently increases engine performance.

2. Nanoparticles act as a catalyst in the combustion process and have a beneficial effect on combustion parameters. The particles increase the momentum density, hence increasing the rate of fuel injection into the combustion chamber, and consequently improving engine performance.

In this study, copper sulfide nanoparticles were used to produce nanofluids. The production of copper sulfide nanoparticles using the microwave method was tested and investigated to find the best power and time and to investigate the effect of surfactants on the size of copper sulfide nanoparticles.

The general advantages of microwave mediated synthesis over conventional ones are (1) reaction rate acceleration as a consequence of high heating rates, (2) wide range of reaction conditions, that is, mild conditions or autoclave conditions, (3) high reaction yields, (4) reaction selectivity due to different microwave absorbing properties, (5) excellent control over reaction conditions, and (6) simple handling, allowing simple and fast optimization of experimental parameters.

Controlling the parameters affecting the synthesis of nanoparticles, including the use of surfactants, pH, experimental environment, reaction temperature, etc., plays an important role in the quality of nanoparticle synthesis. Nanoparticles with smaller size and greater dispersion (non-agglomeration) have higher quality. Surfactants play an important role in the morphological and structural characteristics of the particles formed. Copper sulfide nanoparticles with the smallest particle size according to FE-SEM images were obtained at a power of 500 W and a time of 10 minutes with PEG-400 surfactant as the best surfactant.

Then, the thermal conductivity of nanofluid prepared from copper sulfide with base oil at concentrations of 0.1 and 0.5 wt % was investigated and compared. By reviewing the results obtained, it was concluded that the thermal conductivity in the nanofluid made with copper sulfide in base oil at a concentration of 0.1 percent by weight increased the thermal conductivity by 1.54 percent compared to the thermal conductivity of the base oil, and also in the nanofluid made with copper sulfide and base oil at a concentration of 0.5 percent by weight, the thermal conductivity increased by 3.08 percent compared to the thermal conductivity of the base oil. Since the thermal conductivity of a fluid indicates its ability to absorb and transfer heat, and considering the future of lubricants and the harsher operating conditions, due to factors such as the shrinking volume of engines and the consequent decrease in oil volume and its viscosity, as well as the increase in the operating time of engines at their maximum power, all of which lead to an increase in engine operating temperature and, consequently, an increase in oil temperature, it can be said that if nanoparticles are added to engine oil, in a constant load state, the engine will be able to operate at lower temperatures, and in a constant temperature state, the engine will be able to operate at higher loads or in more severe conditions.

## References

- [1] J. R. Brock, *Nanostructured Materials, Science and Technology*, 1997.
- [2] Moravej, M., Noghrehabadi, A., Esmailinasab, A.L.I. and Khajepour, E., (2020). The effect of SiO<sub>2</sub> nanoparticle on the performance of photovoltaic thermal system: Experimental and Theoretical approach. *Journal of Heat and Mass Transfer Research*, 7(1), 11-24. doi: 10.22075/JHMTR.2020.18904.1254
- [3] Parvar, M., Saedodin, S. and Rostamian, S.H., (2020). Experimental study on the thermal conductivity and viscosity of transformer oil-based nanofluid containing ZnO nanoparticles. *Journal*

*of Heat and Mass Transfer Research*, 7(1), 77-84. doi: 10.22075/JHMTR.2020.19303.1267

- [4] Aminian, M.R., Miroliaei, A.R. and Mirzaei Ziapour, B., (2019). Numerical study of flow and heat transfer characteristics of CuO/H<sub>2</sub>O nanofluid within a mini tube. *Journal of Heat and Mass Transfer Research*, 6(1), 11-20. doi: 10.22075/JHMTR.2018.14156.1205
- [5] Barik, A.K. and Nayak, B., (2017). Fluid flow and heat transfer characteristics in a curved rectangular duct using Al<sub>2</sub>O<sub>3</sub>-water nanofluid. *Journal of Heat and Mass Transfer Research*, 4(2), 103-115. doi: 10.22075/JHMTR.2017.1689.1115
- [6] Mollamahdi, M., Abbaszadeh, M. and Sheikhzadeh, G.A., (2016). Flow field and heat transfer in a channel with a permeable wall filled with Al<sub>2</sub>O<sub>3</sub>-Cu/water micropolar hybrid nanofluid, effects of chemical reaction and magnetic field. *Journal of Heat and Mass Transfer Research*, 3(2), 101- 114. doi: 10.22075/JHMTR.2016.447
- [7] Nath, G. (2018). Physico-Acoustic Study on Thermal Conductivity of Silver Nanofluid. *Journal of Heat and Mass Transfer Research*, 5(2), 105-110. doi: 10.22075/JHMTR.2018.12036.1175
- [8] T. H. Larsen, M. B. Sigman, A. Ghezelbash, R. C. Doty and B. A. Korgel (2003). *J. Am. Chem. Soc.*, 125, 5638.
- [9] Liao, X. H., Chen, N. Y. Sh., and Xu, Sh.B. (2003). A microwave assisted heating method for the preparation of copper sulfide nanorods, *J. Cryst. Growth*, 252, 593-599.
- [10] T, Thongtem; A., Phuruangrat; S. Thongtem (2007). Synthesis and analysis of CuS with different morphologies using cyclic microwave irradiation. *J Mater Sci* 42, 9316-9323.
- [11] Dongke Li , Juanjuan Ma , Lifen Zhou , Ye Li , Changwei Zou, (2015). Synthesis and Characterization of Cu<sub>2</sub>S nano particles by diethyltriamine-assisted hydrothermal method. *Optik*, 126(24), 4971-4973
- [12] S. Gorai, D. Ganguli, S. Chaudhuri, (2004). *Mater. Chem. Phys.* 88, 383-387.

- [13] H.-T. Zhang, G. Wu, X.-H. Chen, (2005). *Langmuir* 21, 4281- 4282.
- [14] Z. Li, W. Chen, H. Wang, Q. Ding, H. Hou, J. Zhang, L. Mi, Z. Zheng, (2011) *Mater. Lett.* 65,1 785-787.
- [15] M. Peng, L.-L. Ma, Y.-G. Zhang, M. Tan, J.-B. Wang, Y. Yu, (2009). *Mater. Res. Bull.* 44, 1834-1841.
- [16] H. Lee, S.W. Yoon, E.J. Kim, J. Park, (2007). *Nano Lett.* 7, 778-784.
- [17] S. Lv, H. Suo, X. Zhao, C. Wang, T. Zhou, S. Jing, Y. Xu, C. Zhao. (2009). *J. Alloys Compd.* 479, 43-46.
- [18] M. Mousavi-Kamazani, M. Salavati-Niasari, (2014). *Composites Part B: Engineering*, 56, 490-496.
- [19] X. Yu, X. An (2010). *Mater. Lett.* 64, 252-254
- [20] Peng, M. L.L., Ma, Zhang, Y.G. and Tan, M. (2009). *Mater. Res. Bull.*, 44, 1834-1841.
- [21] Wu ZC, Pan C, Yao ZY, Zhao QR, Xie Y. (2006). Large-scale synthesis of single-crystal double-fold snowflake Cu<sub>2</sub>S dendrites. *Cryst Growth Des* 6, 1717–9.
- [22] Liu ZP, Xu D, Liang JB, Shen JM, Zhang SY, Qian YT (2005). Growth of Cu<sub>2</sub>S ultrathin nanowires in a binary surfactant solvent. *J Phys Chem B* 109, 10699-704.
- [23] C.M. Ghimbeu, J.-M. Le Meins, C. Zlotea, L. Vidal, G. Schrodj, M. Latroche, C. Vix-Guterl, (2014). Controlled synthesis of NiCo nanoalloys embedded in ordered porous carbon by a novel soft-template strategy, *Carbon*, 67, 260.
- [24] D. Rodríguez-San-Miguel, C. Montoro, F. Zamora, (2020). Covalent organic framework nanosheets: preparation, properties and applications. *Chem. Soc. Rev.* 49 (8), 2291.
- [25] Z. Liu, K. Nie, X. Qu, X. Li, B. Li, Y. Yuan, S. Chong, P. Liu, Y. Li, Z. Yin, W. Huang (2022). General bottom-up colloidal synthesis of nano-monolayer transition-metal dichalcogenides with high 1t'-phase purity. *J. Am. Chem. Soc.*, 144(11) ,4863,

- [26] Y. Fujii, S. Zhou, M. Shimada, M. Kubo. (2023). Synthesis of monodispersed hollow mesoporous organosilica and silica nanoparticles with controllable shell thickness using soft and hard templates. *Langmuir*, 39(13) 4571.
- [27] Y. Liu, J. Goebel, Y. Yin. (2013). Templated synthesis of nanostructured materials. *Chem. Soc. Rev.*, 42(7), 2610.
- [28] Nuha Al-Harbi , Nabil K. Abd-Elrahman (2025). Physical methods for preparation of nanomaterials, their characterization and applications: a review. *Journal of Umm Al-Qura University for Applied Sciences*, 11, 356-377,
- [29] Hussain, R. A.; Hussain, I. (2020). Copper Selenide Thin Films from Growth to Applications. *Solid State Sci.* 100, 106101.
- [30] Chen, M.; Gao, L. (2005). Synthesis and Characterization of Cadmium Selenide Nanorods Via Surfactant-Assisted Hydrothermal Method. *J. Am. Ceram. Soc.* 88, 1643.
- [31] Zhang, Q.; Li, H.; Ma, Y.; Zhai, T. (2016). ZnSe Nanostructures: Synthesis, Properties and Applications. *Prog. Mater. Sci.*, 83, 472-535.
- [32] Chikan, V.; McLaurin, E. (2016). Rapid Nanoparticle Synthesis by Magnetic and Microwave Heating. *Nanomaterials*, 6, 85.
- [33] Sanghi, R. (2000). Microwave Irradiation. *Resonance* 5, 77-81.
- [34] Suwarnkar M.B., Dhabbe R.S., Kadam A.N. and Garadkar K.M. (2014). *Ceram. Int.* 40, 5489.
- [35] N. Elander, J.R. Jones, S.Y. Lu, S. Stone-Elander, (2000). *Chem. Soc. Rev.* 29, 239.
- [36] F. Langa, P. de la Cruz, E. Espildora, J.J. Garcia, M.C. Perez, A. de la Hoz, (2000). *Carbon*, 38, 1641.
- [37] M. Larhed, C. Moberg, A. Hallberg, (2002). *Acc. Chem. Res.* 35, 717.

- [38] Will, H., Scholz, P. and Ondruschka, B. (2002), Heterogene Gasphasenkatalyse im Mikrowellenfeld. *Chemie Ingenieur Technik*, 74, 1057-1067. [https://doi.org/10.1002/1522-2640\(20020815\)74:8<1057::AID-CITE1057>3.0.CO;2-3](https://doi.org/10.1002/1522-2640(20020815)74:8<1057::AID-CITE1057>3.0.CO;2-3).
- [39] J.A. Gerbec, D. Magana, A. Washington, G.F. Strouse, (2005). *J. Am. Chem. Soc.* 127, 15791.
- [40] B. Panzarella, G. Tompsett, W.C. Conner, K. Jones, (2007). *ChemPhysChem* 8, 357.
- [41] Zhou H, Tan X, Huang J and Chen X (2014). *Ceram. Int.* 40, 3688.
- [42] W.C. Conner, G.A. Tompsett, (2008). *J. Phys. Chem. B* 112, 2110.
- [43] Kamarudin N. H. N., Jalil A. A., Triwahyono S., Sazegar M. R., Hamdan S., Baba S. and Ahmad A. (2015). *RSC Adv.* 5, 30023.
- [44] Y. Zhu, X. Guo, J. Jin, Y. Shen, X. Guo, W. Ding, (2007). *J. Mater. Sci.* 42 ,1042-1045.
- [45] Z.P. Liu, D. Xu, J.B. Liang, J.M. Shen, S.Y. Zhang, Y.T. Qian, (2005). *J. Phys. Chem. B.*, 109, 10699.
- [46] B. Klause, G. Bremene, V. Hernn, A. Bosch, (2019). *Experimental and Theoretical Nanotechnology*, 2, 213-220. <https://doi.org/10.56053/3.2.213>